

EFFECT OF DIAZOXIDE ON FRIEDREICH ATAXIA MODELS

Antonella Santoro^{1¶}, Sara Anjomani Virmouni^{2¶}, Eleonora Paradies^{1¶}, Valentina L. Villalobos Coa³, Sahar Al-Mahdawi², Mee Khoo², Vito Porcelli³, Angelo Vozza³, Mara Perrone⁴, Nunzio Denora⁴, Franco Taroni⁵, Giuseppe Merla⁶, Luigi Palmieri^{1,3}, Mark A. Pook², Carlo M.T. Marobbio^{3*}

1. Institute of Biomembranes, Bioenergetics and Molecular Biotechnologies, Consiglio Nazionale delle Ricerche, 70126 Bari, Italy.
2. Department of Life Sciences, College of Health & Life Sciences, Brunel University London, Uxbridge UB8 3PH, UK.
3. Department of Biosciences, Biotechnologies and Biopharmaceutics, University of Bari, 70125, Bari, Italy.
4. Department of Pharmacy - Drug Sciences, University of Bari, 70125 Bari, Italy.
5. Unit of Genetics of Neurodegenerative and Metabolic Diseases, Fondazione IRCCS-Istituto Neurologico Carlo Besta, 20133 Milan, Italy.
6. Medical Genetics Unit, IRCCS Casa Sollievo della Sofferenza, 71013 San Giovanni Rotondo, Italy.

*Carlo M.T. Marobbio, Laboratory of Biochemistry and Molecular Biology, Department of Biosciences, Biotechnologies and Biopharmaceutics, University of Bari, Via Orabona 4, 70125 Bari, Italy. Tel: +39 080 5442791. Fax: +39 080 5442770. Email: carlomarya.marobbio@uniba.it

¶ The authors wish it to be known that, in their opinion, the first three authors should be regarded as joint First Authors.

ABSTRACT

Friedreich ataxia (FRDA) is an inherited recessive disorder caused by a deficiency in the mitochondrial protein frataxin. There is currently no effective treatment for FRDA available, especially for neurological deficits. In this study, we tested diazoxide, a drug commonly used as vasodilator in the treatment of acute hypertension, on cellular and animal models of FRDA. We first showed that diazoxide increases frataxin protein levels in FRDA lymphoblastoid cell lines, via the mTOR pathway. We then explored the potential therapeutic effect of diazoxide in frataxin-deficient transgenic YG8sR mice and we found that prolonged oral administration of 3mpk/d diazoxide was found to be safe, but produced variable effects concerning efficacy. YG8sR mice showed improved beam walk coordination abilities and footprint stride patterns, but a generally reduced locomotor activity. Moreover, they showed significantly increased frataxin expression, improved aconitase activity and decreased protein oxidation in cerebellum and brain mitochondrial tissue extracts. Further studies are needed before this drug should be considered for FRDA clinical trials.

INTRODUCTION

Friedreich ataxia (FRDA, OMIM 229300) is an autosomal recessive disorder due to an increase in the number of GAA trinucleotide repeats within the first intron of the *FXN* gene on chromosome 9 (1). Normal individuals have 5 to 30 GAA repeats, whereas affected individuals have 70 to more than 1000 GAA triplet expansions, causing decreased gene expression. FRDA occurs with a prevalence of approximately 1/50,000 in Caucasian populations and it is characterized clinically by an onset in the first two decades of life with limb ataxia, cerebellar dysarthria, lack of deep-tendon reflexes, pyramidal signs, and sensory loss. Most patients have degeneration of the sensory neurons

in the dorsal root ganglia (DRG) and cerebellum, together with skeletal deformities and hypertrophic cardiomyopathy. There is also an increased incidence of blindness, deafness, and diabetes mellitus, suggesting that the disorder is not limited to the nervous system. The severity of clinical features in FRDA is related to the GAA trinucleotide repeat length (2). Symptoms begin usually in childhood (5–15 years), but onset may vary from infancy to adulthood (3). The *FXN* gene encodes the mitochondrial protein frataxin, which is involved in mitochondrial iron metabolism, assembly of iron-sulphur proteins and heme synthesis (4). The exact physiological function of frataxin is unknown, but there is general agreement that it is involved in cellular iron homeostasis and that its deficiency results in multiple enzyme deficits, mitochondrial dysfunction and oxidative damage (5-7). There is no available effective treatment for FRDA, especially for neurological features. In fact, antioxidant agents, such as idebenone, a short-chain analogue of coenzyme Q10, and iron chelators, which have been used as potential therapeutic agents, ameliorate mitochondrial oxidative stress but have no effects on neurological symptoms (8). Since the disorder is caused by deficiency of *FXN* gene expression, a possible therapeutic strategy could be the stimulation of frataxin expression with exogenous substances to increase its level (9). Several molecules are reported to increase frataxin mRNA or protein levels. However, no clear results supporting a benefit of any of these drugs have so far been obtained in randomized controlled trials (10). Here, we study the effect of diazoxide on cell lines from FRDA patients and on the YG8sR FRDA mouse model (11). Diazoxide is a potassium channel opener, active mainly on the mitochondrial ATP-sensitive potassium channel (mito-KATP channel) (12), which has been in use for over 50 years as a vasodilator in the treatment of acute hypertension (13). It is the active ingredient in Proglycem, a non-diuretic benzothiadiazine derivative taken orally for the management of symptomatic hypoglycaemia (14). Particularly, we studied the effect of diazoxide, to increase frataxin expression levels and to ameliorate the functional and biochemical features of a FRDA mouse model.

RESULTS

Diazoxide induces frataxin expression in FRDA patient lymphoblastoid cells

We analyzed three lymphoblastoid cell lines from FRDA patients (P119, P200, P338) with different GAA repeat expansions, representing: (i) a mild phenotype with late onset and 170/230 GAA repeats (P338); (ii) a canonical phenotype with 500/800 GAA repeats (P119) and (iii) a severe phenotype with early onset and 1100/1100 GAA repeats (P200). As shown in Fig. 1A, the amount of frataxin protein was virtually undetectable in each of the cell extracts (20 μ g). First we test the effect of different diazoxide concentrations on cell viability and we found no toxicity of diazoxide for all cell lines unless they were incubated in the presence of 400 μ M or higher concentrations, for at least 4 days (Fig. 1B). Frataxin expression was measured upon incubating cell cultures in presence of 100 μ M diazoxide (D), 100 μ M diazoxide and 20 mM glucose (GD), or vehicle alone (NT). Cells were collected after 4 days of treatment. We used glucose in combination with diazoxide because the effect of mitoKATP channel openers is exerted only on the ATP-bound potassium channel and depends by the energetic state of the cells (12). Immunoblots of total cell lysates revealed a significant frataxin increase for all cells with D and DG treatments, compared to vehicle-treated cells (NT), ranging from 80 to 300% induction (Fig. 2A-B). The addition of glucose produced minimal increases in frataxin expression compared to diazoxide alone (Fig. 2A). Immunoblots of frataxin from total cell lysates of healthy control cell line revealed no significant differences (Fig. 2C).

Diazoxide induces frataxin expression and decreases oxidative cell damage in YG8sR FRDA mouse model

To test the effect of diazoxide on living organism, we used the YG8sR FRDA mouse model (11). This model is a new line of GAA-repeat-expansion-based FRDA mice derived from YG8R breeding, which contains a single copy of the human *FXN* transgene and a single pure GAA repeat expansion mutation, which was 120 GAA repeats in size in the founder mouse. These mice exhibit an age-dependent GAA repeat expansion accumulation in the CNS, particularly the cerebellum, progressive decrease in motor coordination and significant functional locomotor deficits, features similar to those observed in FRDA patients. In addition, the YG8sR mice exhibit the presence of pathological vacuoles within neurons of the dorsal root ganglia, together with reduced levels of brain aconitase activity, in line with an FRDA-like phenotype. Therefore, these YG8sR mice currently represent the most suitable GAA-repeat-based YAC transgenic mouse model to explore potential FRDA therapies. First, we observed that treatment of YG8sR mice p.o. daily for 5 days with 10 mg/kg diazoxide was safe and no adverse effects were observed with any mice. Since short-term treatment did not produce neither down-stream effects (data not shown), nor an increase of frataxin expression (data not shown) we extended the period of diazoxide treatment to three months. Groups of 20 YG8sR mice (10 male and 10 female, 4 months old) were treated p.o. daily for three months with either vehicle (1% DMSO) or 3mg/kg diazoxide, followed by collection of snap-frozen brain, cerebellum, heart, liver and pancreas tissues. Quantitative RT-PCR (qRT-PCR) analysis of *FXN* mRNA expression of cerebellum and heart tissues from YG8sR mice revealed statistically significant differences between diazoxide-treated and vehicle-treated groups of mice ($p < 0.05$) (Fig. 3A), which translated into 2.6-fold and 1.6-fold increases in *FXN* expression levels, respectively, in diazoxide-treated mice (Fig. 3B).

Similarly, significant 1.4 to 2.8-fold increases in frataxin protein levels were detected by western blot densitometry analysis of mitochondrial extracts from heart ($p < 0.01$), cerebellum ($p < 0.05$) and brain ($p < 0.05$) tissues from YG8sR mice (Fig. 4A-B). We also tested the activity of mitochondrial

aconitase, an iron-sulphur protein involved in iron homeostasis, that is deficient in FRDA cells. A significant increase in aconitase activity, was detected in YG8sR brain tissue ($p < 0.05$), together with trends to increase in other tissues (Fig. 5A). Furthermore, oxyblot analysis revealed a significant reduction ($p < 0.05$) in protein oxidation levels in YG8sR brain, pancreas and liver tissues and trends to decrease in other tissues (Fig. 5B).

Diazoxide effect on functional behaviour of the YG8sR FRDA mouse model

To investigate the ability of oral diazoxide to ameliorate the functional behaviour of the YG8sR FRDA mouse model, groups of 20 mice (10 male and 10 female) were given either 3mg/kg/d diazoxide or vehicle (1% DMSO) p.o. *ad libitum* in drinking water for a period of three months from approximately 4 months of age. This dose of diazoxide was well tolerated and no adverse effects were observed with any mice. Furthermore, there were no significant differences in weight detected between diazoxide-treated (D) and vehicle-treated (V) groups of YG8sR mice (Fig. S1). Functional behavioral studies were performed on all mice, including rotarod analysis (monthly), beam breaker locomotor open field testing (monthly), beam walking (start and end of study), and footprint analysis (start and end of study). Rotarod analysis did not reveal any significant improvement in the performance of YG8sR mice throughout three months of treatment with diazoxide compared with vehicle treatment (Fig. 6A). Beam breaker locomotor analysis identified a general slowing down of movement of diazoxide-treated YG8sR mice compared with vehicle-treated mice from 5-7 months of age, as exemplified by the relative reductions of average velocity (2 way ANOVA $p < 0.01$), no change in the amount of jumping (2 way ANOVA $p < 0.01$), but an increase in the amount of rearing up onto hind limbs, as shown by a relative increase in vertical counts (2 way ANOVA $p < 0.001$) and in vertical time on diazoxide treatment (2 way ANOVA

$p < 0.01$), from month 1 to month 3 of the study (Fig. 6B-E). Beam walk analysis revealed the most significant diazoxide-induced functional effect for YG8sR mice (Fig. 7A). The time taken for mice to cross a 22mm-diameter 90cm-long beam significantly increased over the three-month test period for vehicle-treated YG8sR mice, indicating an increased difficulty in performing this task with age. Interestingly, the time taken to cross the beam significantly decreased over the three-month time period for diazoxide-treated YG8sR mice and there were significant differences between diazoxide-treated and vehicle-treated groups at the three months time point, indicating much improved coordination abilities of YG8sR mice (Fig. 7A). Footprint analysis revealed a significant reduction in the stride length of diazoxide-treated YG8sR mice compared with vehicle-treated YG8sR mice over the three-month test period (Fig. 7B, S1), whereas the hind limb base width for YG8sR mice was not affected by diazoxide treatment (Fig. S1-2).

Diazoxide activates the TOR pathway and promotes nuclear Nrf2 translocation

Literature data showed the ability of diazoxide to activate mTOR kinases (15). To investigate the involvement of the mTOR pathway in the FXN expression, we first analyzed the activation of mTOR kinases in our cell lines. The amount of phosphorylated form of S6K, a target of mTOR kinase (16), was increased after diazoxide treatment (Fig. 8A), confirming the positive effect of 100 μ M diazoxide on mTOR pathway. This increase was almost abolished by the addition of 2 nM rapamycin (Fig. 8A), a well-known inhibitor of mTOR kinases (17). To link this effect to the FXN expression, we analyzed the amount of FXN in diazoxide-induced cell cultures, by using rapamycin. We found that treatment with 2 nM rapamycin completely inhibited the frataxin-increasing effect elicited by diazoxide (Fig. 8B). The antioxidative response exerted by the activation of mTOR pathway has been recently linked to the activation of nuclear factor E2-related factor 2 (NRF2), a transcription factor ubiquitously expressed that regulates cellular redox

homeostasis (18). We observed that induction of frataxin expression is mediated by NRF2 transcription factor, because diazoxide treatment also increased the NRF2 expression in cerebellum tissues of mouse model (Fig. 3). In order to elucidate the effect of diazoxide on the activation of antioxidative pathways exerted by nuclear NRF2 in lymphoblastoid cell lines, we performed an analysis of Nrf2 nuclear translocation. Immunoblotting analysis, 24h after diazoxide treatment, demonstrated an increase of Nrf2 signal in the nuclear fraction of lymphoblastoid cells treated with diazoxide (D) or with diazoxide and glucose (GD) (Fig. 8C-D). We observed a significant increase ($p < 0.05$) of $1.62 \pm 0.20\%$ and $1.66 \pm 0.28\%$ in the relative nNRF2/cNRF2 signals in D and DG samples, respectively (Fig. 8C-D).

DISCUSSION

A number of laboratories have focused on small molecule activators of *FXN* gene expression as potential therapeutic agents. There are several molecules that increase frataxin mRNA or protein levels (9). Due to chromatin structural changes and histone deacetylation, HDAC inhibitors may revert heterochromatin activating the right conformation and restoring the normal function of silenced frataxin gene (19-21). A different strategy is the increase of the amount of frataxin protein by a post-transcriptional mechanism. Recombinant human erythropoietin has been reported to increase the level of frataxin in lymphocytes from FRDA patients and in various human cell lines (22). The molecular basis for this observation is unknown, but it has been proposed to depend on increased stabilization of frataxin protein because the level of frataxin mRNA is the same in treated and untreated control cells. In this study we investigated the possible role of diazoxide on frataxin expression. Diazoxide is a pharmacological agent derived from benzothiazine and it is an activator of the mitochondrial K^+ channels, causing the opening of channels, and in medical practice it is a drug normally used for acute hypertension therapy. Diazoxide activates the mitochondrial ATP-dependent potassium channels (mitoKATP) composed by a potassium channel subunits (Kir6.2)

together with the regulatory subunit sulphonylurea receptor (SUR) (12). These channels can potentially modulate the tightness of coupling between respiration and ATP synthesis, ROS production, mitochondrial dynamics and mitophagy (12 and references therein). MitoKATP is involved in the regulation of mitochondrial ionic homeostasis and, importantly, its activation has been observed to provide cytoprotection against ischemic damage (23, 24). In our study, we tested the effect of diazoxide *in vitro*, using lymphoblastoid cell lines from FRDA patients and *in vivo*, using the YG8sR mouse model. Cells derived from FRDA patients carry the complete frataxin locus together with GAA repeat expansions and regulatory sequences. They are easily accessible and constitute one of the most relevant frataxin-deficient cell models. We used three different cell lines with different number of GAA expansions (170/230 GAA repeats for P338, 500/800 GAA repeats for P119 and 1100/1100 GAA repeats for P200). We used a diazoxide concentration of 100 μ M, which is the approximate human blood concentration of diazoxide after an oral administration of 600 mg (25), and we treated lymphoblastoid cells derived from FRDA patients with diazoxide, alone or in presence of glucose, because the effect of mitoKATP channel openers on mitochondrial function is dependent by the cell's energetic state, activating only the ATP-bound potassium channel (12). We found that diazoxide, alone or in combination with glucose, was able to induce the expression of frataxin protein in all three FRDA cell lines, after 4 days. Preliminary results show that the effect of diazoxide in increased frataxin protein in cell lines is higher after 4 days. We did not observe any increase of protein amount after 1 day, but mRNA increase of FXN expression is detectable after 24 hours (data not shown). The probable mechanism involves activation of the mTOR pathway, since rapamycin treatment of cell cultures completely blocked the ability of diazoxide to significantly enhance the frataxin expression.

The relationship between frataxin expression and the mTOR pathway has recently been revealed by Franco et al. (26). They found that frataxin stimulation by IGF-1 was mediated by the

PI3K/Akt/mTOR pathway. Using either the PI3kinase inhibitor Ly294002, which prevents Akt activation, or rapamycin, the stimulatory action of IGF-1 was blocked. In addition, IGF-1 increases levels of phosphorylated mTOR, an indirect measurement of its activity status, whereas other kinases downstream of the IGF-1 receptor, such as PKC, are not involved in increasing frataxin expression after IGF-1 treatment (26).

We then focused on determining the therapeutic efficacy of diazoxide to increase frataxin expression levels and to ameliorate the functional and biochemical disease effects of a FRDA mouse model. While cell models rarely represent tissue-specific disease features, we used a mouse model with residual frataxin expression, the YG8sR mouse, to investigate the effect of diazoxide in different tissues. These novel GAA-repeat-expansion-based YAC transgenic FRDA mice, which exhibit progressive FRDA-like pathology, represent an excellent model for the investigation of FRDA disease mechanisms and therapy, as they present an increased somatic GAA repeat instability in the brain and cerebellum, together with a significantly reduced expression of frataxin, reduced aconitase activity and a presence of pathological vacuoles in DRG that suggests autophagy of damaged mitochondria (11). We treated the mice with diazoxide by oral administration, because it is known that oral diazoxide crosses the blood-brain barrier fairly rapidly in rats, reaching a plateau by the fourth hour as demonstrated by cerebrospinal fluid analysis (27). Daily dosage of diazoxide was well tolerated and no adverse effects were observed with any of the mice, and at the end of the study. However, unlike lymphoblastoid cell experiments, a 5 day treatment (short-term) did not produce neither an increase of frataxin expression, nor other down-stream effects. By contrast, three months of treatment significantly improved frataxin expression in cerebellum, brain and heart mitochondrial tissue extracts, although the variability in frataxin increase is high amongst different samples. These data suggest that the effect of diazoxide on frataxin expression is not constant and this should be considered for future translational studies. Probably, single dosage of

the treatment could impair the drug effect, and this could also explain different effects observed between short-term treated mice and FRDA cells. In humans for example, diazoxide are metabolized by oxidation and sulfate conjugation and excreted in urine (28). The half-life of diazoxide is about 21 hours, and usual maintenance dosage of 3–8 mg/kg is daily divided in 2 or 3 equal doses every 8 to 12 hours (29 and references therein). Instead, diazoxide concentration in cell culture medium is constant, as it is not metabolized by lymphoblasts. YG8sR mice also showed an increase of aconitase activity, significant only in brain and a significantly decreased protein oxidation in brain, pancreas and liver mitochondrial tissue extracts, but only a trend to decrease in cerebellum and heart tissues. This suggests a different sensitivity of the tissues to oxidative stress, or a different half-life of frataxin that has been degraded through the proteasome (30). Further studies will be required to clarify these differences. Long-term treatment also revealed effects concerning efficacy of diazoxide on functional studies. Beam walk analysis, a test for the coordination abilities, revealed the most significant diazoxide-induced functional effect for YG8sR mice after three months of treatment. Also footprint analysis revealed a significant reduction in the stride length of diazoxide-treated YG8sR mice compared with vehicle-treated YG8sR mice over the three-month test period. Both analyses suggest a positive effect of diazoxide on the coordination abilities. On the contrary, locomotor analysis identified a generally reduced locomotor activity of diazoxide-treated YG8sR mice compared with vehicle-treated mice, although treated mice showed an increase in the amount of rearing up onto hind limbs. This behavior suggests the possible involvement of dopamine receptors that are known to be regulated by KATP channels (31). In fact, mice lacking dopamine D4 receptors show improved coordination abilities but decreased locomotor activity and rearing behavior (32). According to the presence of functional KATP channels on dopaminergic axons, diazoxide treatment suppressed single-pulse evoked dopamine release (31). This adverse effect of diazoxide should be considered for future therapeutic strategy. The hind limb base width and the weight of YG8sR mice was not affected by diazoxide treatment. We observed an

increase in weight in all mice over three months. The increase in weight is observed in FRDA mice in comparison to the healthy control (33). Usually, the increase in weight may be attributed to the decreased locomotor activity of the mice, but Tomassini et al. found that increase of FXN expression and amelioration in locomotor activity and motor coordination due to IFN γ treatment, occurred independently of body weight changes (34).

Our results suggest that the protective effects of diazoxide mediated by a stimulatory effect on frataxin expression, as observed in cell culture experiments and in brain and cerebellum of YG8sR tissues, are sufficient to ameliorate the coordination abilities. Neuroprotective effects of diazoxide have been well documented in conditions of ischemia and hypoxia (35, 36). It has been shown to promote myelination in the neonatal brain and attenuate hypoxia-induced brain injury in neonatal mice (37) as well as oligodendrocyte differentiation in neonatal mouse brain (38).

The involvement of the mTOR signaling pathway as a possible mechanism by which diazoxide can induce frataxin expression is confirmed by the increase of S6K phosphorylation and by the treatment of rapamycin that completely inhibited the frataxin-increasing effect elicited by diazoxide (16). Kwon et al. found that (^3H)thymidine incorporation in adult rodent islets chronically exposed to glucose is largely mediated through mTOR via the KATP channel, and 250 μM diazoxide enhanced the ability of elevated glucose to stimulate cell proliferation and S6K1 phosphorylation, a known target of mTOR kinases (15). The authors also demonstrated that 25 nM rapamycin completely inhibited the effect of diazoxide. A possible downstream target of mTOR signalling could be the NRF2 transcription factor mediated pathway. Activation of the NRF2 pathway induces frataxin expression as demonstrated by Sahdeo and colleagues (39). They found seven potential Nrf2-binding sites (AREs) between 20 kb upstream and 5 kb downstream of the FXN locus, three of them, located upstream of the transcription start site for FXN, with excellent ARE scores. They demonstrated by chromatin Immunoprecipitation (ChIP) experiments that they are active and

functional Nrf2-binding sites (39). The increase of frataxin protein may be achieved, at least in part, by a transcriptional mechanism, since qRT-PCR analysis of *FXN* mRNA revealed increases in expression of cerebellum and heart tissues from YG8sR mice, together with increases in Nrf2 expression. We also demonstrated that activation of the mTOR pathway in diazoxide-treated cell lines induces Nrf2 nuclear translocation, and this process is inhibited by rapamycin. Our data are in agreement with a recent study by Virgili and colleagues who showed that diazoxide prevents endogenous oxidative damage of NSC-34 motoneurons after different neurotoxic insults and increases Nrf2 nuclear translocation (40). This study suggests that diazoxide is able to induce FXN expression in human cells from FRDA patients and in brain, cerebellum and heart tissues of YG8sR mice. Positive effects have also been observed on oxidative stress protection and coordination abilities of treated mice but further studies are needed to clarify the variable effects concerning functional studies.

MATERIAL AND METHODS

Cell lines and culture conditions

Human control and FRDA lymphoblastoid cell lines were maintained in RPMI 1640 supplemented with 8 mM glutamine, 2 mM sodium pyruvate, 1x non-essential amino acids, 15% foetal bovine serum, and 100 U/ml penicillin and 0.1 mg/ml streptomycin. All cell lines were cultured at 37°C in a humidified atmosphere containing 5% CO₂ in 25 cm² culture flasks (kept in an upright position). Antibiotics were omitted during pharmacological compound assays. Cells were treated for 4 days with 100 µM diazoxide, alone or combined with 20 mM glucose or 2 nM rapamycin. Medium with reagents were changed every day during the treatment period. Nrf2 level was determined in nuclear

protein extracts from lymphoblastoid cell cultures 24 h after treatments, using 4 wells from 24-well plates for each experimental condition.

Cytotoxicity Assay

Potential cytotoxic effects of diazoxide were carried out on lymphoblastoid cell lines using MTT (3-[4,5-dimethylthiazol-2-yl]-2,5 diphenyl tetrazolium bromide) assay. Cells were seeded into 6 well plates at a density of 2.5×10^5 cells per well in 1 mL of RPMI medium and incubated for 4 days in 5% CO₂ environment at 37 °C. The assay is based on the mitochondrial activity of living cells to convert water soluble MTT into water insoluble formazan crystals due to the reductive activity of mitochondria. Cells were incubated for 4 days in the presence of the test agent at four dilutions ranging from 50 to 400 µM. The assay was carried out as elsewhere described (15, 41). The experiment was carried out in triplicate, after 4 days.

Tissue processing

Homogenate of each tissue was prepared suspending 200 mg of tissue in a buffer containing 250 mM sucrose, 1 mM EGTA and 10 mM TRIS pH7.4 and using a Teflon glass potter. Cell debris was pelleted by centrifugation at 800xg and discarded. Mitochondria from tissue homogenates were harvested by centrifugation at 13,000xg for 12 min at 4 °C. Mitochondria enriched pellets was then stored at -80 °C until further processing.

Quantitative reverse transcriptase PCR

Total RNA was isolated from the mouse tissues by homogenisation with Trizol (Invitrogen), followed by DNase I treatment, and cDNA was then prepared by using AMV reverse transcriptase (Invitrogen) with oligo (dT)₂₀ primers and quantified by Nanodrop (ThermoScientific) analysis (42). Levels of human transgenic *FXN* or mouse *Nrf2* mRNA expression were assessed by qPCR using an Quant Studio 7 detection system and SYBR[®] Green (Applied Biosystems) with the following primers: (1) *FXN*: FRT-I forward 5'-TTGAAGACCTTGCAGACAAG-3' and RRT-II reverse 5'-AGCCAGATTTGCTTGTTTGG-3', 121 bp amplicon size; (2) *Nrf2*: forward 5'-TTTTCCATTCCCGAATTACAGT-3' and reverse 5'-GGAGATCGATGAGTAAAAATGGT-3', 126 bp amplicon size. For each sample, assays were performed in triplicate.

Western blot analysis

Lymphoblastoid cells were washed three times, lysed with cell lysis buffer (0.15 M NaCl, 5 mM EDTA, 1% NP-40, 10 mM Tris-Cl, pH 7.4) and transferred to a microcentrifuge tube. For *Nrf2* analysis, cytoplasmic and nuclear fractions were separated by using the NE-Nuclear and Cytoplasmic Extraction kit (Thermo Fisher) by following the manufacturer's protocol. Protein concentration was determined using the BCA protein assay reagent (Thermo Scientific). 20 µg of mouse mitochondrial protein or 80 µg of human cell proteins were separated on BOLT BIS-TRIS PLUS 12% polyacrylamide gels (43) and electroblotted onto nitrocellulose membranes (Thermo Fisher). Membranes were washed 20 min with TBST buffer and incubated with anti-frataxin (Santa Cruz Biotechnology, 1:500), anti-*Nrf2* (Thermo Fisher, 1:500), anti-S6K1 (phospho T389; 1:500), anti-laminA (BD Bioscience, 1:500), anti-βATPase (BD Bioscience, 1:10,000) primary antibodies. Anti-NRF2, anti-laminA and anti-frataxin were incubated for 12 hours at 4°C. Anti-βATPase and anti-S6K were incubated for 1 h at RT. Membranes were washed three times with TBS for 15 min, and then incubated for 1h at RT with anti-mouse (Pierce, 1:10,000) and anti-rabbit (Pierce, 1:5,000)

HRP secondary antibodies (Thermo Fisher). Finally, membranes were washed three times with TBS and immunoreactive bands were visualized using Immobilon Western Chemiluminescent HRP Substrate (Millipore)(44). The intensity of protein bands was quantified by using QuantityOne 4.6.3 Image software (ChemiDoc XRS; Bio-Rad) and normalized against proper loading controls (45, 46).

Quantification of mitochondrial protein oxidation

Carbonylated mitochondrial proteins were detected using the OxyBlot Protein Oxidation Detection Kit (MILLIPORE). 2,4 dinitrophenylhydrazine- derivatized crude mitochondrial protein extracts (10 µg) were dot blotted, incubated with a primary antibody against DNP-hydrazone followed by a horseradish peroxidase-conjugated secondary antibody, visualized using the ECL chemiluminescent detection method and quantified by densitometry (47).

Enzymatic assays

Citrate synthase activity was determined following the rate of 5,5'-dithiobis-(2-nitrobenzoic) acid (DTNB) consumption, as described (48). The CoA produced in the reaction mix reacts with the DTNB to form 5-thio-2-nitrobenzoic acid (TNB), a yellow product observed spectrophotometrically by measuring absorbance at 412 nm. 10 µg of mitochondrial proteins from each tissue were used for spectrophotometric assay using Cary win 50 UV- Spectrophotometer. Aconitase activities were determined according to the method described previously (23). Briefly, mitochondria were lysed in Tris-HCl (pH 7.4) containing 0.5% Triton X-100 and 2.5 mM sodium citrate, for 5 minutes on ice. Insoluble material was removed by centrifugation (14000 x g, 40 sec), and protein concentration was determined with Bradford reagent (Bio-Rad, Milan, Italy). 100-300 µg of mitochondrial extract

were added to a substrate mix (50 mM Tris/HCl pH 7.4, 0.2 mM NADP⁺, 5 mM Na citrate, 0.6 mM MgCl₂, 0.1% (v/v) Triton X-100 and 1-2 units of isocitrate dehydrogenase) and the reactions were incubated at 25°C for 15 minutes, followed by spectrophotometric absorbance measurements at 340 nm. In samples of low aconitase activity, an initial lag in NADPH formation is seen, probably due to a delayed accumulation of cis-aconitate (49). Thus, the determinations of aconitase activity were determined using linear rates during the latter half of a 60-min assay.

Animal procedures and behavioural assessments

YG8sR mice were assessed from 4 months of age for a period of 3 months. Weight determination, rotarod performance and beam breaker locomotor performance were assessed monthly, while beam walk performance and footprint analysis were assessed at the start and end of the test period, using previously described methodology (11). All procedures were carried out in accordance with the UK Home Office Animals Scientific Procedures Act (1986) and with ethical approval from the Brunel University London Animals Welfare and Ethical Review Board.

Statistical analysis

Statistical analysis was performed using the paired Student's *t* test when comparing two groups or a two-way ANOVA when comparing multiple groups. Differences with $p < 0.05$ were assumed to be significant. In the figures, $p < 0.05$, $p < 0.01$ and $p < 0.001$ were marked with *, ** and ***, respectively.

ACKNOWLEDGEMENTS

We are grateful to the Genomic and Genetic Disorders Biobank, Telethon Network of Genetic Biobanks (Telethon Italy grant GTB12001G), and of the EuroBioBank network for biospecimens banking. This work was supported by funding from the Friedreich's Ataxia Research Alliance (FARA); and the Italian Ministry of Health [Ricerca Corrente 2014–16] to G.M.; and “5 × 1000” voluntary contributions to G.M.

Conflict of Interest statement. Santoro A., Palmieri L. and Marobbio C.M.T. filed a U.S. patent: Diazoxide for the treatment of Friedreich's Ataxia. US 8,716,250 B2, Università degli Studi di Bari. Merla G. is a paid consultant for Takeda Pharmaceutical Company.

REFERENCES

1. Campuzano, V., Montermini, L., Moltò, M.D., Pianese, L., Cossée, M., Cavalcanti, F., Monros, E., Rodius, F., Duclos, F., Monticelli, A., et al. (1996) Friedreich's ataxia: autosomal recessive disease caused by an intronic GAA triplet repeat expansion. *Science*, **271**, 1423-1427.
2. Filla, A., De Michele, G., Cavalcanti, F., Pianese, L., Monticelli, A., Campanella, G. and Coccozza, S. (1996) The relationship between trinucleotide (GAA) repeat length and clinical features in Friedreich ataxia. *Am. J. Hum. Genet.*, **59**, 554-560.
3. Mateo, I., Llorca, J., Volpini, V., Corral, J., Berciano, J. and Combarros, O. (2003) GAA expansion size and age at onset of Friedreich's ataxia. *Neurology*, **61**, 274-275.

4. Napier, I., Ponka, P. and Richardson, D.R. (2005) Iron trafficking in the mitochondrion: novel pathways revealed by disease. *Blood*, **105**, 1867-1874.
5. Dürr, A., Cossee, M., Agid, Y., Campuzano, V., Mignard, C., Penet, C., Mandel, J.-L., Brice, A. and Koenig, M. (1996) Clinical and genetic abnormalities in patients with Friedreich's ataxia. *N. Engl. J. Med.*, **335**, 1169–1175.
6. Pandolfo, M. (2006) Iron and Friedreich ataxia. *J. Neural. Transm. Suppl.*, **70**, 143-146.
7. Lu, C. and Cortopassi, G. (2007) Frataxin knockdown causes loss of cytoplasmic iron–sulfur cluster functions, redox alterations and induction of heme transcripts. *Arch. Biochem. Biophys.*, **457**, 111–122.
8. Fogel, B.L. and Perlman, S. (2007) Clinical features and molecular genetics of autosomal recessive cerebellar ataxias. *Lancet Neurol.*, **6**, 245-257.
9. Gottesfeld, J.M. (2007) Small molecules affecting transcription in Friedreich ataxia. *Pharmacol. Ther.*, **116**, 236-248.
10. Pandolfo, M. (2013) Treatment of Friedreich's ataxia. *Expert Opin. Orphan Drugs*, **1**, 221-234.
11. Anjomani Virmouni, S., Ezzatizadeh, V., Sandi, C., Sandi, M., Al-Mahdawi, S., Chutake, Y. and Pook, M.A. (2015) A novel GAA-repeat-expansion-based mouse model of Friedreich's ataxia. *Dis. Model. Mech.*, **8**, 225-235.
12. Szabò, I., Leanza, L., Gulbins, E. and Zoratti, M. (2012) Physiology of potassium channels in the inner membrane of mitochondria. *Pflugers Arch.*, **463**, 231-246.
13. Hutcheon, D.E., Harman, M.A. and Schwartz, M.I. (1962) Diazoxide in the treatment of hypertension. *J. New Drugs*, **2**, 292-297.
14. Samols, E. and Marks, V. (1966) The treatment of hypoglycaemia with diazoxide. *Proc. R. Soc. Med.*, **59**, 811-814.

15. Kwon, G., Marshall, C.A., Liu, H., Pappan, K.L., Remedi, M.S., McDaniel, M.L. (2006) Glucose-stimulated DNA synthesis through mammalian target of rapamycin (mTOR) is regulated by KATP channels: effects on cell cycle progression in rodent islets. *J. Biol. Chem.*, **281**, 3261-3267.
16. Magnuson, B., Ekim, B. and Fingar, D.C. (2012) Regulation and function of ribosomal protein S6 kinase (S6K) within mTOR signalling networks. *Biochem. J.*, **441**, 1-21.
17. Wullschleger, S., Loewith, R. and Hall, M.N. (2006) TOR signaling in growth and metabolism. *Cell*, **124**, 471-484.
18. Lim, J.L., Wilhelmus, M.M., de Vries, H.E., Drukarch, B., Hoozemans, J.J. and van Horsen, J. (2014) Antioxidative defense mechanisms controlled by Nrf2: state-of-the-art and clinical perspectives in neurodegenerative diseases. *Arch. Toxicol.*, **88**, 1773–1786.
19. Bidichandani, S.I., Ashizawa, T. and Patel, P.I. (1998) The GAA triplet-repeat expansion in Friedreich ataxia interferes with transcription and may be associated with an unusual DNA structure. *Am. J. Hum. Genet.*, **62**, 111–121.
20. Di Prospero, N.A. and Fischbeck, K.H. (2005) Therapeutics development for triplet repeat expansion diseases. *Nat. Rev. Genet.*, **6**, 756-765.
21. Sandi, C., Pinto, R.M., Al-Mahdawi, S., Ezzatizadeh, V., Barnes, G., Jones, S., Rusche, J.R., Gottesfeld, J.M. and Pook, M.A. (2011) Prolonged treatment with pimelic o-aminobenzamide HDAC inhibitors ameliorates the disease phenotype of a Friedreich ataxia mouse model. *Neurobiol. Dis.*, **42**, 496–505.
22. Sturm, B., Stupphann, D., Kaun, C., Boesch, S., Schranzhofer, M., Wojta, J., Goldenberg, H. and Scheiber–Mojdehkar, B. (2005) Recombinant human erythropoietin: effects on frataxin expression in vitro. *Eur. J. Clin. Invest.*, **35**, 711-717.

23. Bernardi, P. (1999) Mitochondrial transport of cations: channels, exchangers, and permeability transition. *Physiol. Rev.*, **79**, 1127–1155.
24. Costa, A.D.T. and Garlid, K.D. (2009) MitoKATP activity in healthy and ischemic hearts. *J. Bioenerg. Biomembr.*, **41**, 123–126.
25. Calesnick, B., Katchen, B. and Black, J. (1965) Importance of dissolution rates in producing effective diazoxide blood levels in man. *J. Pharm. Sci.*, **54**, 1277-1280.
26. Franco, C., Fernández, S. and Torres-Alemán, I. (2012) Frataxin deficiency unveils cell-context dependent actions of insulin-like growth factor I on neurons. *Mol. Neurodegener.*, **7**, 1-10.
27. Kishore, P., Boucai, L., Zhang, K., Li, W., Koppaka, S., Kehlenbrink, S., Schiwiek, A., Esterson, Y.B., Mehta, D., Bursheh, S., et al. (2011) Activation of K(ATP) channels suppresses glucose production in humans. *Clin. Invest.*, **121**, 4916-4920.
28. American Society of Health-System Pharmacists (2015) Diazoxide. In McEvoy, G.K. (ed.), *AHFS drug information*. Bethesda, United States.
29. Friciu, M., Zarea, S., Roullin, V.G. and Leclair, G. (2016) Stability of diazoxide in extemporaneously compounded oral suspensions. *PLoS One*, **11**, 1-12.
30. Rufini, A., Fortuni, S., Arcuri, G., Condo, I., Serio, D., Incani, O., Malisan, F., Ventura, N. and Testi, R. (2011) Preventing the ubiquitin-proteasome-dependent degradation of frataxin, the protein defective in Friedreich's ataxia. *Hum. Mol. Genet.*, **20**, 1253–1261.
31. Patel, J.C., Witkovsky, P., Coetzee, W.A. and Rice M.E. (2011) Subsecond regulation of striatal dopamine release by pre-synaptic KATP channels. *J. Neurochem.*, **118**, 721-736.
32. Rubinstein, M., Phillips, T.J., Bunzow, J.R., Falzone, T.L., Dziewczapolski, G., Zhang, G., Fang, Y., Larson, J.L., McDougall, J.A., Chester, J.A., et al. (1997) Mice lacking dopamine D4 receptors are supersensitive to ethanol, cocaine, and methamphetamine. *Cell*, **90**, 991-1001.

33. Anjomani Virmouni, S., Sandi, C., Al-Mahdawi, S. and Pook, M.A. (2014) Cellular, molecular and functional characterisation of YAC transgenic mouse models of Friedreich ataxia. *PLoS ONE*, **9**, 1-13.
34. Tomassini, B., Arcuri, G., Fortuni, S., Sandi, C., Ezzatizadeh, V., Casali, C., Condò, I., Malisan, F., Al-Mahdawi, S., Pook, M.A. et al. (2012) Interferon gamma upregulates frataxin and corrects the functional deficits in a Friedreich ataxia model. *Hum. Mol. Genet.* **21**, 2855-2861.
35. Domoki, F., Perciaccante, J.V., Veltkamp, R., Bari, F. and Busija, D.W. (1999) Mitochondrial potassium channel opener diazoxide preserves neuronal-vascular function after cerebral ischemia in newborn pigs. *Stroke*, **30**, 2713-2718.
36. Shake, J.G., Peck, E.A., Marban, E., Gott, V.L., Johnston, M.V., Troncoso, J.C., Redmond, J.M. and Baumgartner, W.A. (2001) Pharmacologically induced preconditioning with diazoxide: a novel approach to brain protection. *Ann. Thorac. Surg.*, **72**, 1849-1854.
37. Fogal, B., McClaskey, C., Yan, S., Yan, H.L. and Rivkees, S.A. (2010) Diazoxide promotes oligodendrocyte precursor cell proliferation and myelination. *PLoSOne*, **5**, 1-9.
38. Zhu, Y., Wendler, C.C., Shi, O. and Rivkees, S.A. (2014) Diazoxide promotes oligodendrocyte differentiation in neonatal brain in normoxia and chronic sublethal hypoxia. *Brain Res.*, **1586**, 64-72.
39. Sahdeo, S., Scott, B.D., McMackin, M.Z., Jasoliya, M., Brown, B., Wulff, H., Perlman, S.L., Pook, M.A. and Cortopassi, G.A. (2014) Dyclonine rescues frataxin deficiency in animal models and buccal cells of patients with Friedreich's ataxia. *Hum. Mol. Genet.*, **23**, 6848-6862.
40. Virgili, N., Mancera, P., Wappenhans, B., Sorrosal, G., Biber, K., Pugliese, M. and Espinosa-Parrilla, J.F. (2013) K(ATP) channel opener diazoxide prevents

- neurodegeneration: a new mechanism of action via antioxidative pathway activation. *PLoS One*, **8**, 1-11.
41. Laquintana, V., Denora, N., Lopalco, A., Lopodota, A., Cutrignelli, A., Lasorsa, F.M., Agostino, G. and Franco, M. (2014) Translocator protein ligand-plga conjugated nanoparticles for 5-fluorouracil delivery to glioma cancer cells. *Mol. Pharm.*, **11**, 859–871.
42. Kishita, Y., Pajak, A., Bolar, N.A., Marobbio, C.M.T., Maffezzini, C., Miniero, D.V., Monné, M., Kohda, M., Stranneheim, H., Murayama, K. et al. (2015) Intra-mitochondrial Methylation Deficiency Due to Mutations in SLC25A26. *Am. J. Hum. Genet.*, **97**, 761-768.
43. Giannuzzi, G., Lobefaro, N., Paradies, E., Vozza, A., Punzi, G. and Marobbio, C.M.T. (2014) Overexpression in *E. coli* and purification of the *L. pneumophila* Lpp2981 protein. *Mol. Biotechnol.*, **56**, 157-165.
44. Marobbio, C.M.T., Punzi, G., Pierri, C.L., Palmieri, L., Calvello, R., Panaro, M.A. and Palmieri, F. (2015) Pathogenic potential of SLC25A15 mutations assessed by transport assays and complementation of *Saccharomyces cerevisiae* ORT1 null mutant. *Mol. Genet. Metab.*, **115**, 27-32.
45. Ersoy Tunalı, N., Marobbio, C.M.T., Tiryakioğlu, N.O., Punzi, G., Saygılı, S.K., Onal, H. and Palmieri, F. (2014) A novel mutation in the SLC25A15 gene in a Turkish patient with HHH syndrome: functional analysis of the mutant protein. *Mol. Genet. Metab.*, **112**, 25-29.
46. Lunetti, P., Damiano, F., De Benedetto, G., Siculella, L., Pennetta, A., Muto, L., Paradies, E., Marobbio, C.M.T., Dolce, V. and Capobianco, L. (2016) Characterization

- of Human and Yeast Mitochondrial Glycine Carriers with Implications for Heme Biosynthesis and Anemia. *J. Biol. Chem.*, **291**, 19746-19759.
47. Marobbio, C.M.T., Pisano, I., Porcelli, V., Lasorsa, F.M. and Palmieri, L. (2012) Rapamycin reduces oxidative stress in frataxin-deficient yeast cells. *Mitochondrion*, **12**, 156-166.
48. Blomstrand, E., Rådegran, G. and Saltin, B. (1997) Maximum rate of oxygen uptake by human skeletal muscle in relation to maximal activities of enzymes in the Krebs cycle. *J. Physiol.*, **501**, 455-460.
49. Gardner, P.R., Nguyen, D.D. and White, C.W. (1994) Aconitase is a sensitive and critical target of oxygen poisoning in cultured mammalian cells and in rat lungs. *Proc. Natl. Acad. Sci. U.S.A.*, **91**, 12248-12252.

FIGURE LEGENDS

Fig 1. 100 μ M diazoxide is not toxic for FRDA lymphoblastoid cells. (A) Immunoblot of FXN from 20 μ g total cell lysates of lymphoblasts of three FRDA patients (P119, P200, P338) and healthy control (C). Subunit β of ATP synthase was used as loading control. (B) Cell viability of lymphoblasts cells lines. Lymphoblasts from three FRDA patients (P119, P200, P338) were treated for 4 days with different diazoxide concentrations. Results demonstrated that 100 μ M diazoxide is not toxic for cells. Results expressed as mean \pm SD (* $p < 0.05$, ** $p < 0.01$ Student's t test, $n=4$).

Fig 2. Diazoxide induces FXN in cultured FRDA lymphoblastoid cells. (A) Lymphoblasts from three FRDA patients (P119, P200, P338) were incubated in presence of 100 μ M diazoxide (D), 100

μ M diazoxide and 20 mM glucose (GD), or vehicle alone (0.1% DMSO) (NT). Total protein was collected after 4 days, and lysates (80 μ g) were probed by western blot analysis for FXN expression and normalized to subunit β of ATP synthase. The plotted data represent the mean fold change in FXN protein in drug-treated cells, normalized to vehicle control (* p <0.05, ** p <0.01 Student's t test, n =4). (B) and (C) Representative blots are shown for FRDA patient (B) or healthy control (C) lymphoblast cell lines treated as above.

Fig 3. Diazoxide induces FXN and NRF2 expression in YG8sR cerebellum and heart tissues.

QRT-PCR analysis of transgenic *FXN* and *NRF2* mRNA levels in YG8sR cerebellum and heart tissues. Expression data (A) and fold changes (B) of *FXN* and *NRF2* mRNA levels of diazoxide-treated tissues (D) relative to those of vehicle-treated tissues (V), using the formula $x=2^{(\Delta Ct)}$ and adjusting for input cDNA concentrations.

Fig 4. Diazoxide induces FXN in YG8sR cerebellum, brain and heart tissues. (A) Tissues from a group of treated (n =8) or untreated (n =8) mice were analyzed for the FXN protein expression. 20 μ g mitochondrial protein extracts from cerebellum (C), brain (B), heart (H), pancreas (P) and liver (L) tissues of YG8sR mice treated with p.o. daily for three months with either vehicle (1% DMSO) (open bars) or 3mg/kg diazoxide (grey bars) were probed by western blot analysis for FXN expression and normalized to subunit β of ATP synthase. The plotted data represent the mean fold change in FXN protein in drug-treated tissues, normalized to vehicle control in three independent experiments (** p <0.01, * p <0.05 Student's t test, n =3). (B) A representative blot is shown for cerebellum (C), brain (B), heart (H), pancreas (P) and liver (L) tissues of YG8sR mice treated as above.

Fig 5. Diazoxide decreases oxidative stress in YG8sR mice. (A) Mitochondria purified from brain, heart, pancreas and liver tissues of YG8sR mice treated with p.o. daily for three months with either vehicle (1% DMSO) (open bars) or 3mg/kg diazoxide (grey bars) were tested (A) for aconitase activity (**p<0.01, Student's t test, n=3), or (B) for oxyblot analysis (**p<0.01, Student's t test, n=3).

Fig 6. Diazoxide reduces locomotor activity of YG8sR mice. (A) Rotarod performance of mice, measured at monthly intervals. (B-E) Beam breaker locomotor analysis at monthly intervals, measured as fold changes in performance from month 1 to month 3. B: average velocity; C: jump counts; D: vertical counts; E: vertical time. Each parameter was measured four times for each mouse (*p<0.05, ***p<0.001, Student's t test, n=20).

Fig 7. Diazoxide improves YG8sR mice coordination. (A) Beam walk analysis, determining the average times taken for mice to cross a 22mm diameter beam, before and after diazoxide or vehicle treatment. (B) Footprint analysis, determining the average stride length of mice, before and after diazoxide or vehicle treatment. Each parameter was measured four times for each mouse (*p<0.05, ***p<0.001, Student's t test, n=20).

Fig 8. Diazoxide induces FXN expression through mTOR pathway and NRF2 nuclear translocation in cultured FRDA lymphoblastoid cells. (A) The induction of mTOR pathway exerted by diazoxide was tested by treating lymphoblast cell lines from FRDA patient (P200) with

100 μ M diazoxide (D), 100 μ M diazoxide and 20 mM glucose (DG), 100 μ M diazoxide, 20 mM glucose and 2nM rapamycin (DGR), or vehicle alone (0.1% DMSO) (NT). 20 μ g of proteins from cellular or nuclear fractions were separated by SDS-PAGE and transferred to nitrocellulose membranes and probed for phosphorylated form of S6K and normalized to subunit β of ATP synthase. (B) To test if the mTOR kinases are involved in the mechanism of FXN induction, lymphoblast cell lines from FRDA patient (P200) were treated with 100 μ M diazoxide and 20 mM glucose (GD), 100 μ M diazoxide, 20 mM glucose and 2nM rapamycin (GDR), 100 μ M diazoxide (D), 100 μ M diazoxide and 2nM rapamycin (DR), or vehicle alone (0.1% DMSO) (NT). Total protein was collected after 4 days, and lysates were probed by western blot analysis for FXN expression and normalized to subunit β of ATP synthase. (C) For the analysis of Nrf2 nuclear translocation, lymphoblast cell lines from FRDA patient (P200) were treated with 100 μ M diazoxide (D), 100 μ M diazoxide and 20 mM glucose (DG), or vehicle alone (0.1% DMSO) (NT) for 24 h. Cellular and nuclear fractions were normalized to subunit β of ATP synthase and laminA, respectively. (D) The ratio of Nrf2 nuclear and cellular content of samples treated as above was calculated and displayed in the histograms (* p <0.05, Student's t test, n =3).

S1 Fig. Weight of YG8sR mice (n=20).

S2 Fig. Footprint images. Representative images of the footprint analysis at baseline and post-treatment time points are shown. The scale bar = 1cm.

S3 Fig. Footprint analysis. Hind limb base width of YG8sR mice before and after diazoxide or vehicle treatment (n=20). Representative images of the footprint analysis at baseline and post-treatment time points are shown in S2 Fig. The scale bar = 1cm.

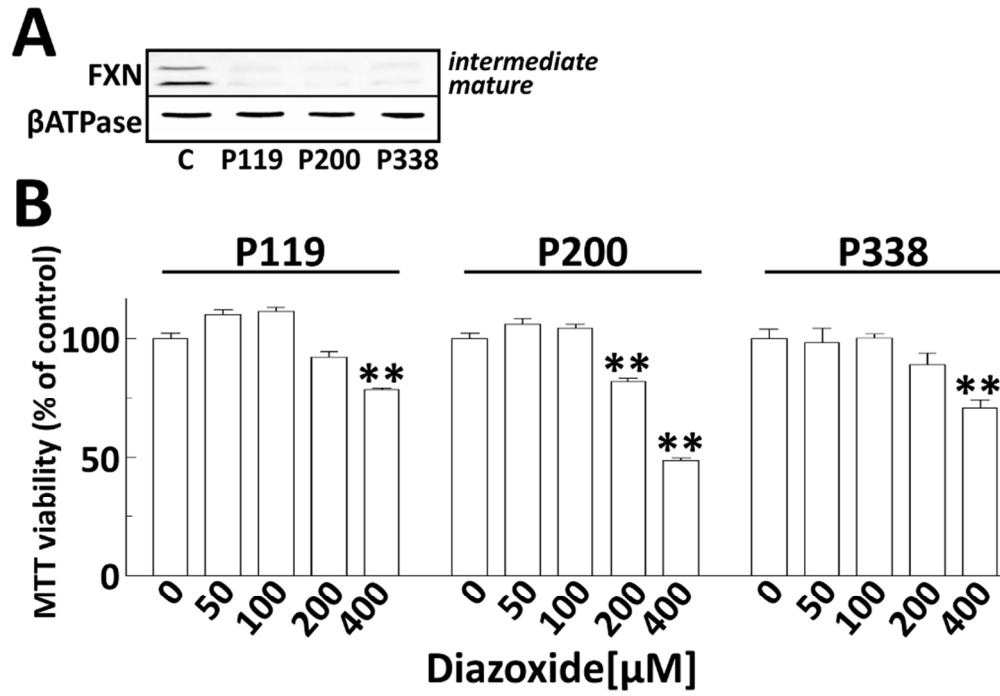


Fig 1. 100 μM diazoxide is not toxic for FRDA lymphoblastoid cells.

86x59mm (300 x 300 DPI)

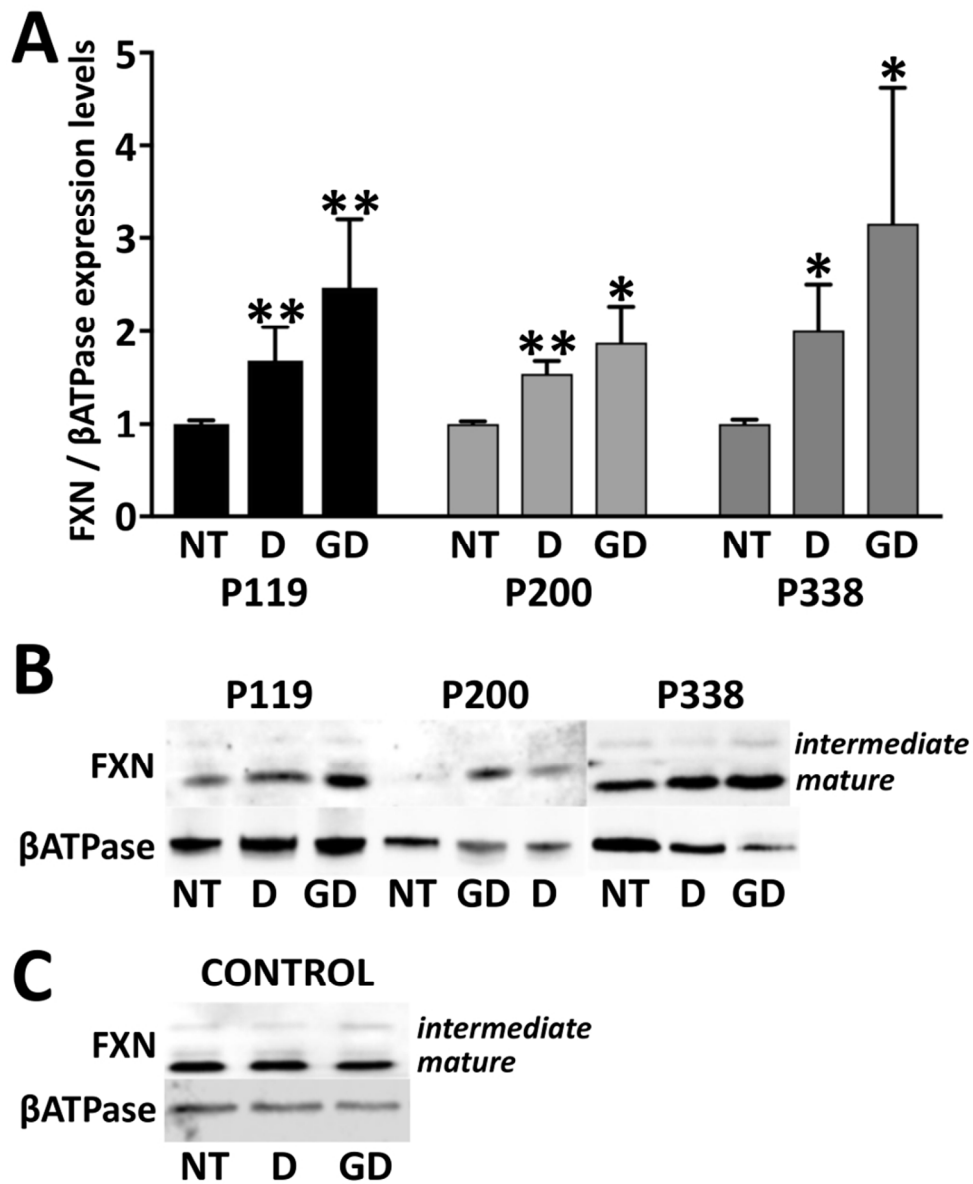


Fig 2. Diazoxide induces FXN in cultured FRDA lymphoblastoid cells.

86x106mm (300 x 300 DPI)

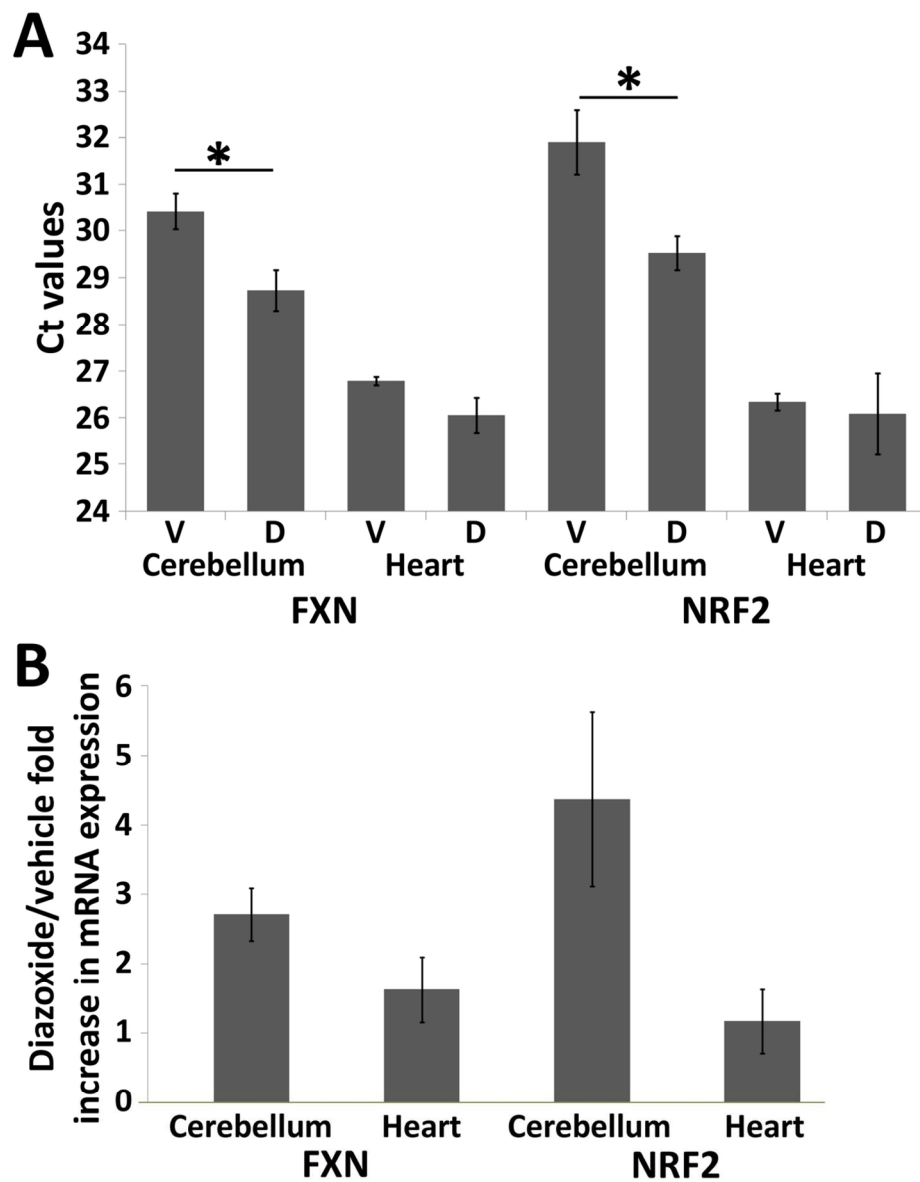


Fig 3. Diazoxide induces FXN and NRF2 expression in YG8sR cerebellum and heart tissues.

111x143mm (300 x 300 DPI)

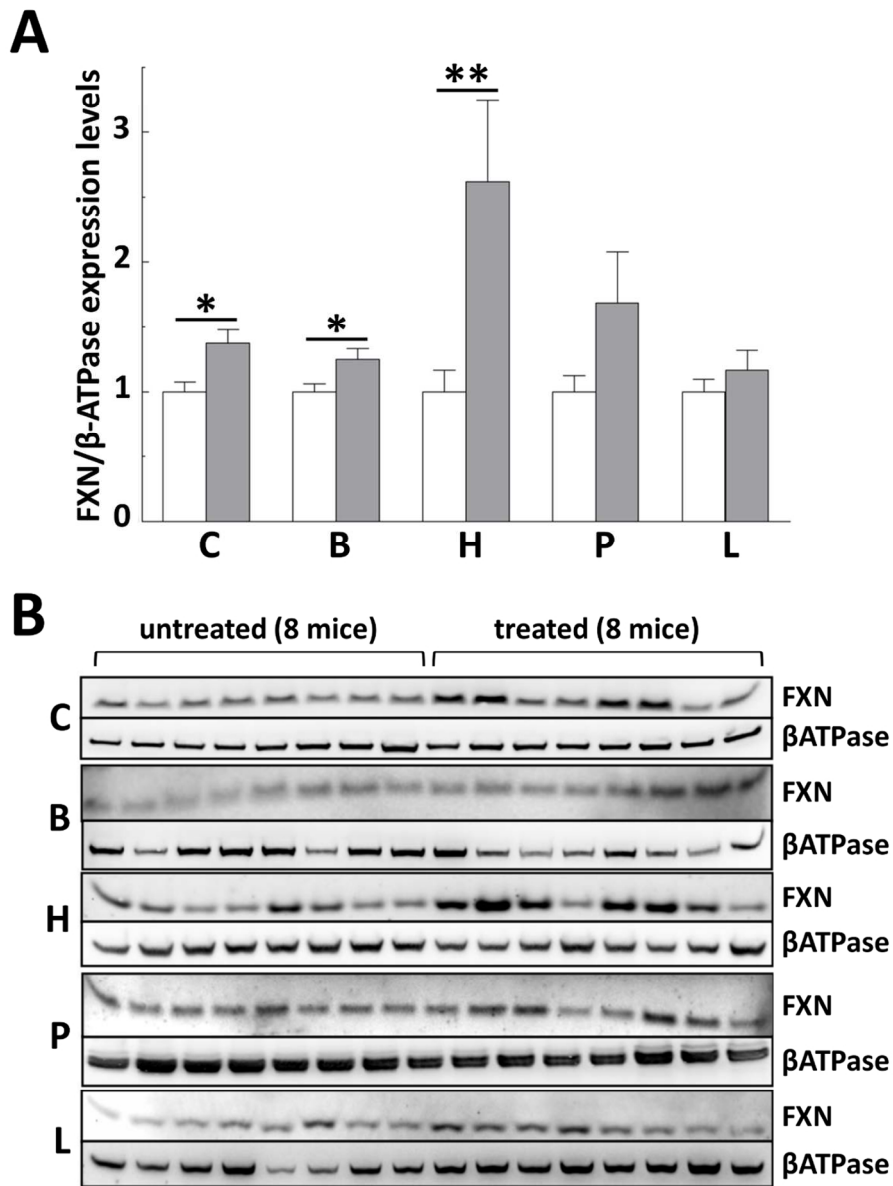


Fig 4. Diazoxide induces FXN in YG8sR cerebellum, brain and heart tissues.

104x140mm (300 x 300 DPI)

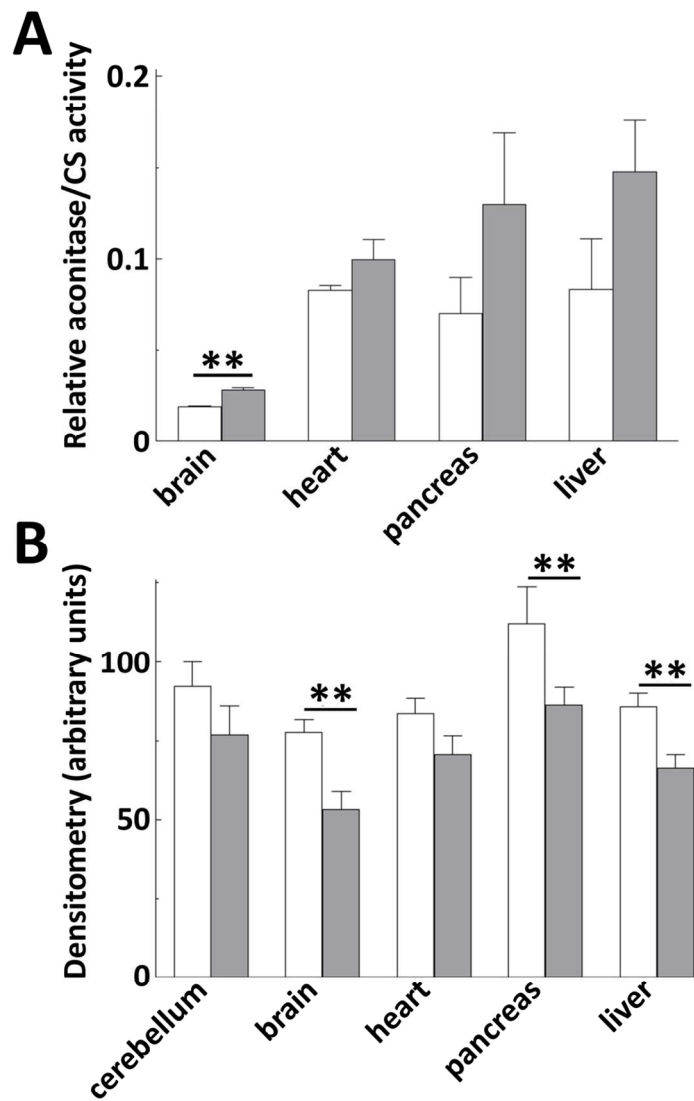


Fig 5. Diazoxide decreases oxidative stress in YG8sR mice.

114x152mm (300 x 300 DPI)

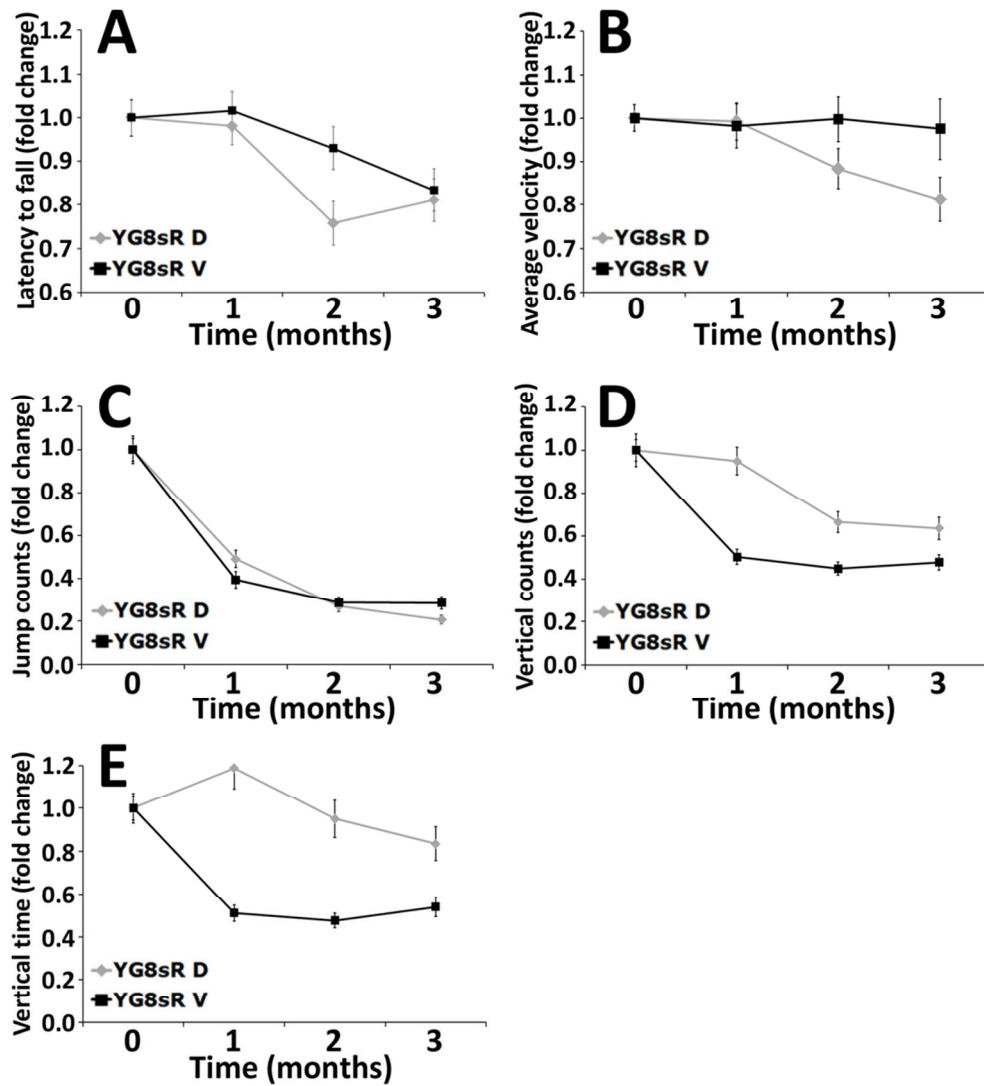


Fig 6. Diazoxide reduces locomotor activity of YG8sR mice.

93x102mm (300 x 300 DPI)

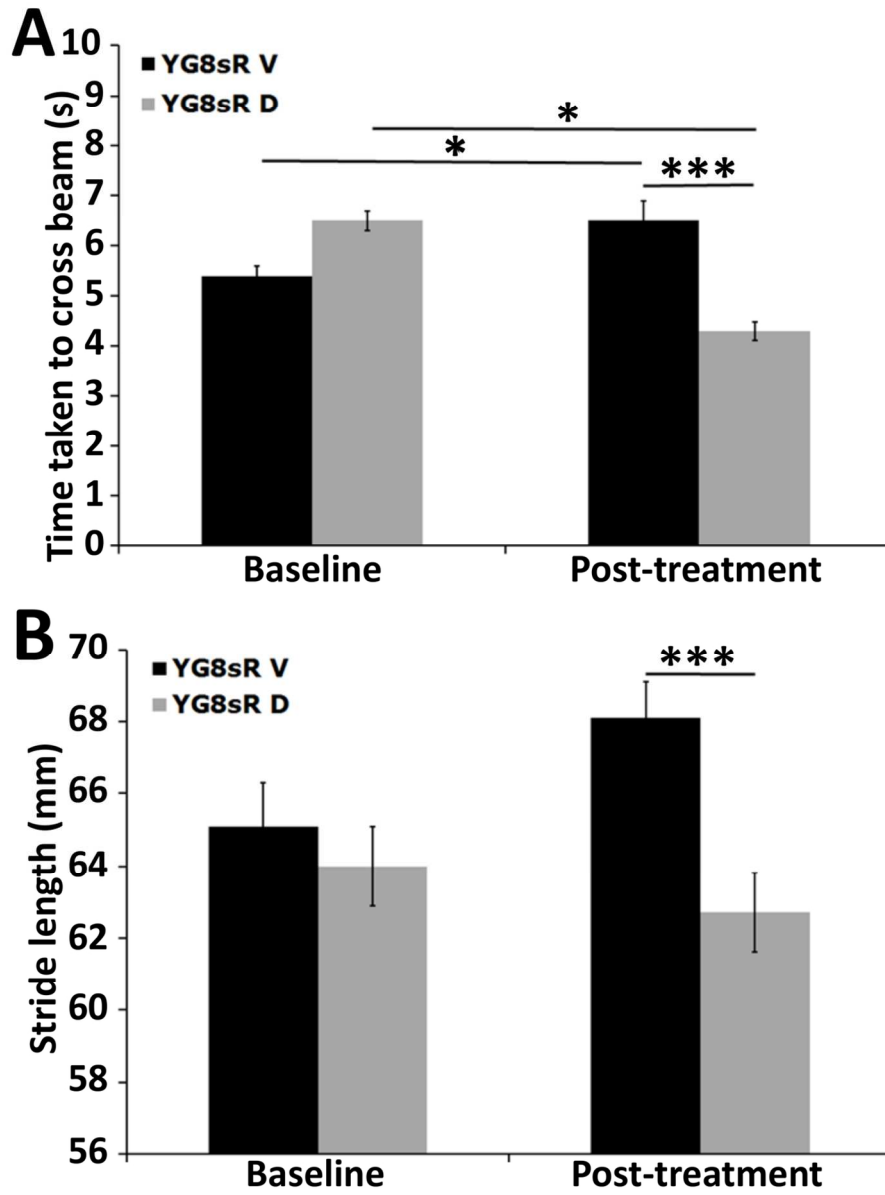


Fig 7. Diazoxide improves YG8sR mice coordination.

114x152mm (300 x 300 DPI)

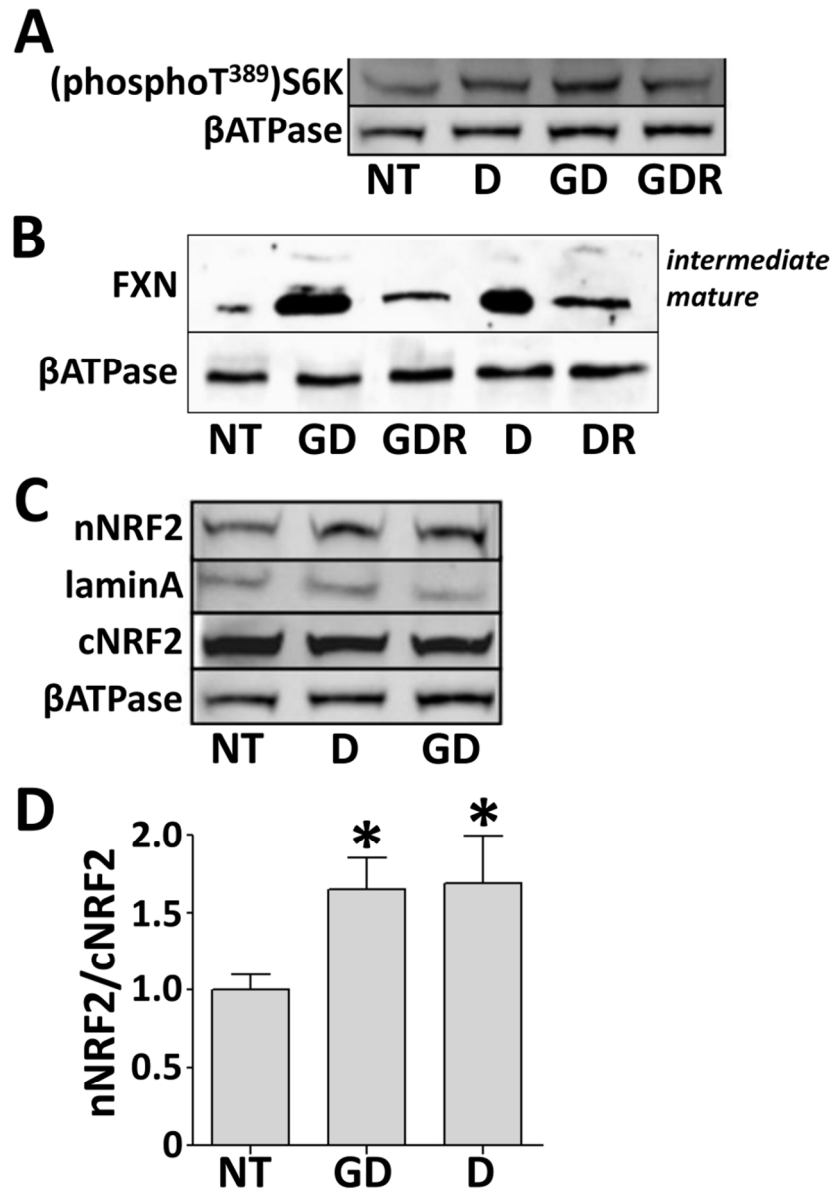


Fig 8. Diazoxide induces FXN expression through mTOR pathway and NRF2 nuclear translocation in cultured FRDA lymphoblastoid cells.

86x123mm (300 x 300 DPI)